NeuroImage: Clinical 32 (2021) 102845

Contents lists available at ScienceDirect

NeuroImage: Clinical

journal homepage: www.elsevier.com/locate/ynicl

Salience network glutamate and brain connectivity in medication-naïve first episode patients – A multimodal magnetic resonance spectroscopy and resting state functional connectivity MRI study

Jose O. Maximo [a], Frederic Briend [a,b], William P. Armstrong [a], Nina V. Kraguljac [a], Adrienne C. Lahti [a,*]

[a] Department of Psychiatry and Behavioral Neurobiology, University of Alabama at Birmingham, Birmingham, AL, USA
[b] UMR1253, iBrain, Université de Tours, Inserm, Tours, France

ARTICLE INFO

Keywords:
First episode psychosis
Medication-naïve
Functional connectivity
Glutamate
Brain network
Dorsal anterior cingulate

ABSTRACT

Background: Salience network (SN) connectivity is altered in schizophrenia, but the pathophysiological origin remains poorly understood. The goal of this multimodal neuroimaging study was to investigate the role of glutamatergic metabolism as putative mechanism underlying SN dysconnectivity in first episode psychosis (FEP) subjects.

Methods: We measured glutamate + glutamine (Glx) in the dorsal anterior cingulate cortex (dACC) from 70 antipsychotic-naïve FEP subjects and 52 healthy controls (HC). The dACC was then used as seed to define positive and negative resting state functional connectivity (FC) of the SN. We used multiple regression analyses to test main effects and group interactions of Glx and FC associations.

Results: dACC Glx levels did not differ between groups. Positive FC was significantly reduced in FEP compared to HC, and no group differences were found in negative FC. Group interactions of Glx-FC associations were found within the SN for positive FC, and in parietal cortices for negative FC. In HC, higher Glx levels predicted greater positive FC in the dACC and insula, and greater negative FC of the lateral parietal cortex. These relationships were weaker or absent in FEP.

Conclusions: Here, we found that positive FC in the SN is already altered in medication-naïve FEP, underscoring the importance of considering both correlations and anticorrelations for characterization of pathology. Our data demonstrate that Glx and functional connectivity work differently in FEP than in HC, pointing to a possible mechanism underlying dysconnectivity in psychosis.

1. Introduction

Resting state functional connectivity (FC), the temporal correlation of brain activity at rest between different regions using functional magnetic resonance imaging (fMRI), has consistently identified (Williamson and Allman, 2012) large scale brain networks found to be heavily implicated in higher-order cognitive processes including the default mode (DMN), salience (SN), central executive (CEN), and dorsal attention (DAN) networks (Menon, 2011). The SN, which includes two hubs, the dorsal anterior cingulate cortex (dACC) and the insula, is responsible for guiding the allocation of neuronal processing, stimuli, and energy resources in the brain (Menon, 2011). For example, switching between the internally directed cognition of the DMN and the externally directed cognition of the CEN. In schizophrenia, this failure to integrate stimuli (misattribution of experiences) is thought to be responsible for hallucinations and delusions (Kapur, 2003). Altered functional activation during cognitive tasks and functional connectivity during rest have been consistently reported in this network (Cadena et al., 2019, 2018a, 2018b; Kerns et al., 2005; Kraguljac et al., 2016; Minzenberg et al., 2009; Overbeek et al., 2019; Reid et al., 2010). However, the pathophysiological origin of this altered activation and connectivity remains poorly understood.

Disruptions in glutamate metabolism in the dACC have been reported in postmortem and MRS studies in schizophrenia. For example,

* Corresponding author at: Department of Psychiatry and Behavioral Neurobiology, University of Alabama at Birmingham, SC 501, 1530 3rd Ave South, Birmingham, AL 35294-0017, USA.
E-mail address: alahti@uabmc.edu (A.C. Lahti).

https://doi.org/10.1016/j.nicl.2021.102845
Received 3 July 2021; Received in revised form 8 September 2021; Accepted 25 September 2021
Available online 29 September 2021

Roberts et al. (2020) used electron microscopy in dACC postmortem samples and identified decreases in the number of both excitatory and inhibitory synaptic connections. These alterations in synaptic connections are thought to be responsible for elevated levels in glutamate observed in schizophrenia (Merritt et al., 2016). An increasing number of magnetic resonance spectroscopy (MRS) studies in schizophrenia, including studies investigating the dACC, suggest altered glutamate metabolism in vivo. Because of the considerable heterogeneity of these studies definite conclusions are difficult to draw (Egerton et al., 2017; Merritt et al., 2016), but it seems clear that stage of illness (Stone et al., 2009), functional status of the recruited sample (Dempster et al., 2020), acuity of illness (Pan et al., 2021), magnet strength (3 T vs. 7 T) (Sydnor and Roalf, 2020), and medication status (de la Fuente-Sandoval et al., 2013; Kraguljac et al., 2019; Kraguljac et al., 2012) are affecting MRS measurements.

Consistent with its role in neuroenergetics (Shulman et al., 2014; Singh, 2012), recent studies have revealed that cortical glutamate appears to play an important role in modulating the blood-oxygen level-dependent (BOLD) signal (Enzi et al., 2012; Kraguljac and Lahti, 2021) as well as the functional connectivity between brain regions (Kraguljac et al., 2017; Tomasi et al., 2013). In addition, a review of combined MRS/fMRI studies in healthy subjects concluded that there was evidence that cortical glutamate was not only correlated with the BOLD signal within the measured voxels, but also with regions distant from the voxel (Duncan et al., 2014). In schizophrenia, a handful of studies have now reported a pattern of altered coupling between glutamate measured in a voxel prescribed in the dACC and the BOLD response in regions distinct from the dACC (Cadena et al., 2018a; Falkenberg et al., 2014; Limongi and Jeon et al., 2020; Limongi et al., 2021; McCutcheon et al., 2021; Overbeek et al., 2019). However, these studies enrolled both chronic (Cadena et al., 2018a; Falkenberg et al., 2014), medicated first episode psychosis (FEP) patients (Overbeek et al., 2019) and unmedicated FEP patients (Limongi et al., 2020, 2021; McCutcheon et al., 2021), thus the link between these abnormalities remains somewhat scattered in the schizophrenia literature.

The goal of this combined fMRI/MRS neuroimaging study was to investigate the role of glutamatergic metabolism underlying functional connectivity within the SN in medication-naïve FEP. To this end, we compared a group of medication-naïve FEP patients and matched healthy controls (HC) on measures of dACC glutamate + glutamine (Glx) levels and resting state FC of the SN. Based on previous findings from our group (Cadena et al., 2019, 2018a, 2018b; Kraguljac et al., 2016; Kraguljac et al., 2013; Overbeek et al., 2019), we hypothesized that dACC Glx levels would be higher in FEP than HC, and reduced FC in FEP compared to HC between the dACC and the rest of the SN would be found. We further hypothesized that the correlation between dACC Glx levels and SN FC would be different between the groups, suggesting an abnormal inhibition/excitation balance in FEP. We also conducted exploratory analyses to investigate associations between FC of regions showing differential Glx-effects in patients and clinical variables.

1.1. Materials and methods

1.1.1. Participants

A total of 127 (HC = 54; FEP = 73) subjects participated in this study. FEP patients were recruited from outpatient clinics, inpatient units and the emergency room at the University of Alabama at Birmingham (UAB). Studies were approved by the University of Alabama at Birmingham Institutional Review Board, and written informed consent was obtained before enrollment [patients had to be deemed competent to provide consent and parental consent was obtained for patients under the age of 18] (Carpenter et al., 2000). Patient were considered eligible for participation if they were between 14 and 55 years old, reported symptoms consistent with a psychotic disorder (e.g., hallucinations, delusions, negative symptoms), and were interested in study participation. Exclusion criteria were major neurological or medical conditions, history of significant head trauma, substance use disorders (excluding nicotine and cannabis) within 1 month of imaging, more than five days of lifetime antipsychotic exposure, pregnancy or breastfeeding, and MRI contraindications. Use of concomitant medications was permitted as clinically indicated. The use of antidepressants was not an exclusion criterion, nonetheless, only a few participants were taking medication at baseline. We did not exclude patients based on a pre-specified maximal duration of untreated psychosis before study entry. Consensus diagnoses were made according to DSM-5 criteria by two board certified psychiatrists from all historical and direct assessment information available (ACL and NVK). Because of the longitudinal design of the study (ClinicalTrials.gov Identifier: NCT02034253, NCT03442101) clinical observations over several months of follow up were used to establish a final diagnosis. The Brief Psychiatric Rating Scale (BPRS) and Repeatable Battery for the Assessment of Neuropsychological Status (RBANS) were used to assess symptom severity and cognition (Overall and Gorham, 1962; Randolph et al., 1998). We also recruited HC who were matched on age, gender, and parental socioeconomic status (SES). In addition to above outlined criteria, HCs with a personal history or a family history of a psychiatric illness in a first-degree relative were also excluded.

The dataset here has subject overlap with our recent reports (Briend et al., 2020; Kraguljac et al., 2020, 2021; Maximo et al., 2020; Nelson et al., 2020). Data for NCT 034420101 is deposited to the NDA data archive and shared per NIMH agreement.

1.1.2. Data acquisition

All imaging was performed on a 3T whole-body Siemens MAGNETOM Prisma MRI scanner equipped with a 20-channel head coil. A high-resolution T1-weighted structural scan was acquired for anatomical reference and spectroscopic voxel placement (MPRAGE: TR = 2400 ms; TE = 2.22 ms; inversion time = 1000 ms; flip angle = 8°; GRAPPA factor = 2; voxel size = 0.8 mm^3). MRS data were collected from a voxel in dACC (27 × 20 × 10 mm^3; Fig. 1A). Slices were aligned to anatomical midline to control for head tilt. The MRS voxel was placed in a region of the bilateral dorsal ACC above the genu of the corpus callosum on the basis of the sagittal and coronal images (Fig. 1A).

Following automatic and manual shimming to optimize field homogeneity across the voxel, chemical shift selective (CHESS) pulses were used to suppress the water signal. Then, spectra were obtained using a Point Resolved Spectroscopy Sequence (PRESS; TR/TE = 2000/80 ms, flip angle = 90°, vector size 1024, 96 averages (Mullins et al., 2008; Schubert et al., 2004)). Moreover, eight averages of unsuppressed water scans with the same acquisition parameters were acquired for quantify metabolites with respect to internal water.

Finally, two resting state functional MRI (fMRI) data runs were acquired in opposing phase encoding directions (anterior > posterior and posterior > anterior; TR = 1550 ms; TE = 37.80 ms; flip angle = 71°, FOV = 104 mm^2; multi-band acceleration factor = 4; voxel size = 2 mm^3; 225 volumes, and 72 axial slices). Subjects were instructed to look at a fixation cross, keep their eyes open, and let their mind wander.

1.1.3. Data preprocessing

1.1.3.1. Magnetic resonance spectroscopy data. All spectra were analyzed in jMRUI version 6.0 using the AMARES algorithm (Vanhamme et al., 1997). Prior knowledge derived from in vitro and in vivo spectra was included in the model. A phantom solution of 20 mM glutamate in buffer (30 mM sodium hydrogen carbonate and 30 mM sodium carbonate; pH, 7.1) was imaged using the same acquisition parameters from the in vivo study. The model consisted of peaks for N-Acetyl aspartate (NAA), choline (Cho), Creatine (Cr + Cr2), Glx was modeled as a triplet (large peak with 2 small outer wings) as previously described (Kraguljac et al., 2013). After removing the residual water peak using the Hankel-Lanczos singular values decomposition filter, the amplitude of the center Glx peak was estimated and Glx levels were

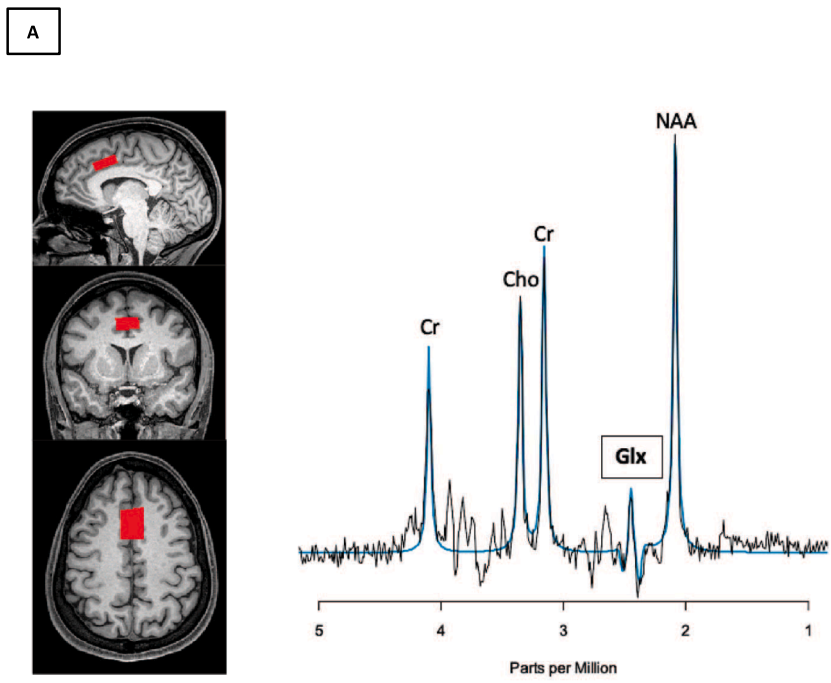

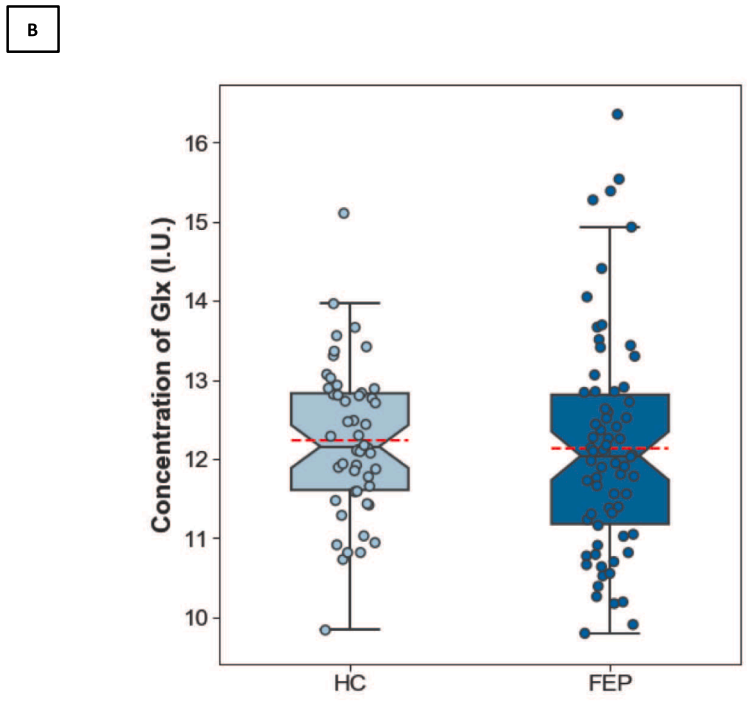

Fig. 1. A) Example voxel placement in the dorsal anterior cingulate cortex in one subject and its spectrum. The black line is a collected spectrum and the blue line is a model fit; B) Boxplot of Glx levels in antipsychotic-naïve FEP compared to HC. Each dot corresponds to one participant. The red line indicates the mean dACC Glx level for each group. HC, healthy controls; FEP, first episode psychosis; Cr, creatine; Cho, choline; Glx, glutamate + glutamine; NAA, N-acetyl aspartate; dACC, dorsal anterior cingulate cortex; and I.U., institutional unit. (For interpretation of the references to colour in this figure legend, the reader is referred to the web version of this article.)

calculated relative to the unsuppressed voxel water and expressed in institutional units (I.U.) (Scheidegger et al., 2013). Metabolite levels were corrected for partial volume effects (i.e. gray and white matter voxel content) according to Gasparovic and colleagues (Gasparovic et al., 2006; Gussew et al., 2012); the fraction of cerebrospinal fluid, gray and white matter were calculated by segmentation of the T1-weighted images in SPM8.

Exclusion criteria for Glx were failure of the fitting algorithm, signal to noise ratio (SNR) < 3, full width at half maximum (FWHM) > 0.1 ppm (Wilson et al., 2019), and Cramer-Rao lower bounds (CRLB) $> 20\%$.

1.1.3.2. Resting state fMRI data. After discarding the first 10 volumes on each fMRI run allowing for signal equilibration, susceptibility artifacts were corrected using spin echo field maps in FSL's topup (Jenkinson et al., 2012), and then the 2 corrected fMRI runs were concatenated resulting in a single 4D image of 430 total volumes. Data were then preprocessed and analyzed using the CONN toolbox version 20b [https://web.conn-toolbox.org, (Whitfield-Gabrieli and Nieto-Castanon, 2012)]. Functional images were slice-timing and motion-corrected using rigid-body realignment, co-registered to the structural image, normalized to Montreal Neurological Institute (MNI) space, bandpass filtered

(0.008 < f < 0.08 Hz), and spatially smoothed with a 4-mm full width at half maximum Gaussian (FWHM) kernel.

Framewise displacement (FD) and percentage of censored data were then calculated. Motion outliers as detected by the Artifact Detection Tools toolbox (NeuroImaging Tools and Resources Collaboratory, https://www.nitrc.org/projects/artifact_detect/) were censored (composite volume-to-volume motion > 0.5 mm and intensity > 3 SDs), and the six motion parameters derived from rigid-body realignment and their derivatives, as well as the first 5 component time series derived from CSF and white matter using aCompCor and corresponding derivatives, were regressed out from the signal. No global signal regression was performed as the correlation between global signal and Glx was not significant (r = -0.02, p = 0.84) and as this can impact functional connectivity analyses (Murphy et al., 2009).

1.1.3.3. Statistical analyses. We performed a one-way ANCOVA controlling for age, gender, and smoking status to compare dACC Glx levels between groups using the Statistical Package for Social Sciences (SPSS, IBM Corp. Released 2017. IBM SPSS Statistics for macOS, Version 25.0. Armonk, NY: IBM Corp.).

For positive and negative FC analyses, the dACC region of interest (ROI) within the CONN toolbox was used to calculate functional connectivity. Residual timeseries from the dACC ROI were extracted and correlated with every other voxel in the brain, thus creating individual whole-brain z-transformed correlation maps. To restrict all analyses strictly to the SN, a mask was created by thresholding average positive correlation maps for each group at t-value of 10 and a cluster size of 100 voxels (Supplementary Fig. 1A). An additional analysis of negative FC [anticorrelations, (Goelman et al., 2014)] was also performed. Negative FC maps of the SN were also computed for each network and thresholded at a negative t-value of 20 and a cluster size of 100 (Supplementary Fig. 1B). Then, intersection masks were created. Group analyses were then performed within each positive and negative mask (p < 0.01 using threshold-free cluster enhancement [TFCE, (Smith and Nichols, 2009)]. TFCE correction estimates a voxel-wise metric that captures the amount of cluster-like local spatial support for an activation, combined with non-parametric permutation testing for inference. Age, sex, and FD were treated as covariates.

To examine how Glx plays a role with FC, dACC Glx values were entered into a regression analysis to predict FC while controlling for age, gender, and FD. Data were entered into 2nd-level analyses and tested for group interaction effects (how Glx-FC associations differ between HC and FEP). This was done for both positive and negative FC analyses. Multiple comparisons correction was performed as described above.

Finally, as exploratory analyses, dACC Glx scores and BPRS subscales scores (positive, negative, and total) were correlated. FC from clusters of significant FC group differences (clusters from Fig. 2) and Glx-FC group interactions (clusters from Fig. 3A and B) BPRS subscales scores were also correlated.

1.2. Results

1.2.1. Demographics and clinical data

After excluding five subjects with noisy MRS data, seven subjects with missing data/scans (did not have resting state scans), and seven subjects with excessive head motion (<50% of data remaining after censoring or volume-to-volume motion > 0.5 mm), our sample included 122 (HC = 52; FEP = 70) for MRS analysis and 113 for FC analyses (HC = 52; FEP = 61).

Demographic data are summarized in Table 1. HC and FEP were well matched in terms of age, gender and SES. However, they differed in smoking status (Table 1).

1.2.2. Glx concentration levels

There was not a significant group difference in dACC Glx levels between HC (M = 12.24, SD = 0.96) and FEP (M = 12.14, SD = 1.39) after

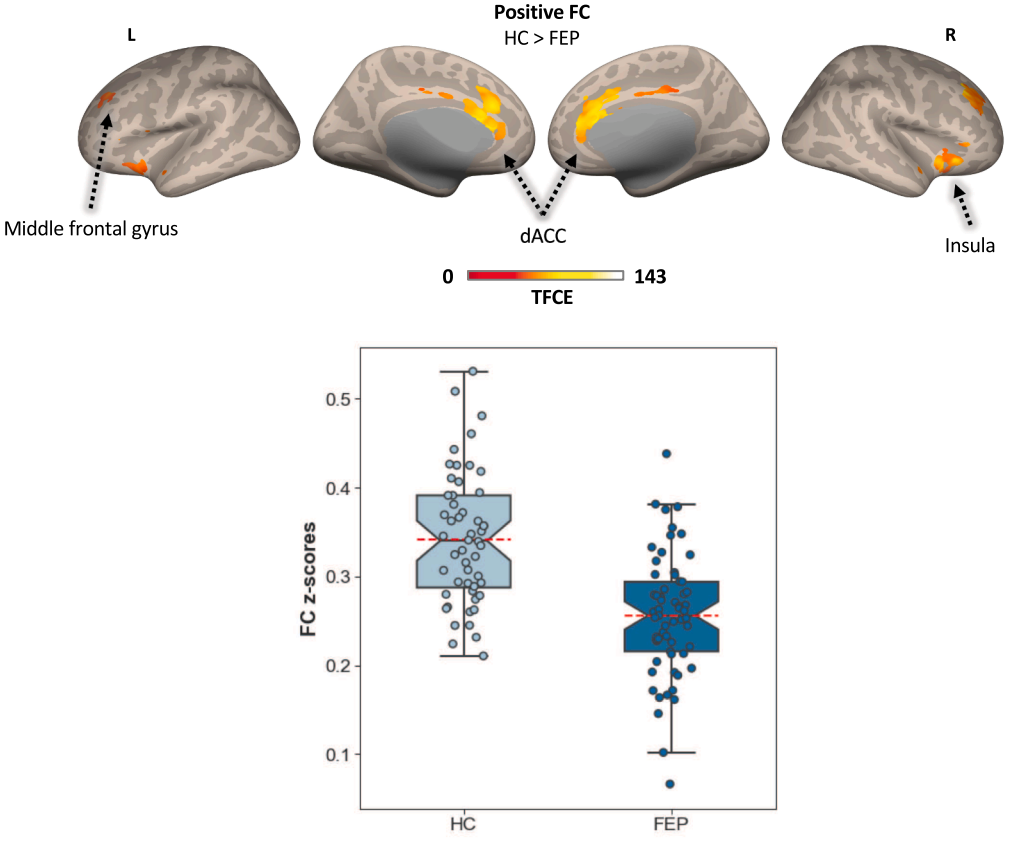

Fig. 2. A) Clusters of significant group differences in positive FC which indicate HC > FEP. Boxplot of FC where each dot corresponds to one participant. The red line indicates the mean FC value for each group. Clusters of significant group differences were combined and FC was extracted for data visualization purposes on the scatterplot below. All analyses were TFCE corrected. HC, healthy controls; FEP, first episode psychosis; FC, functional connectivity; dACC, dorsal anterior cingulate cortex. (For interpretation of the references to colour in this figure legend, the reader is referred to the web version of this article.)

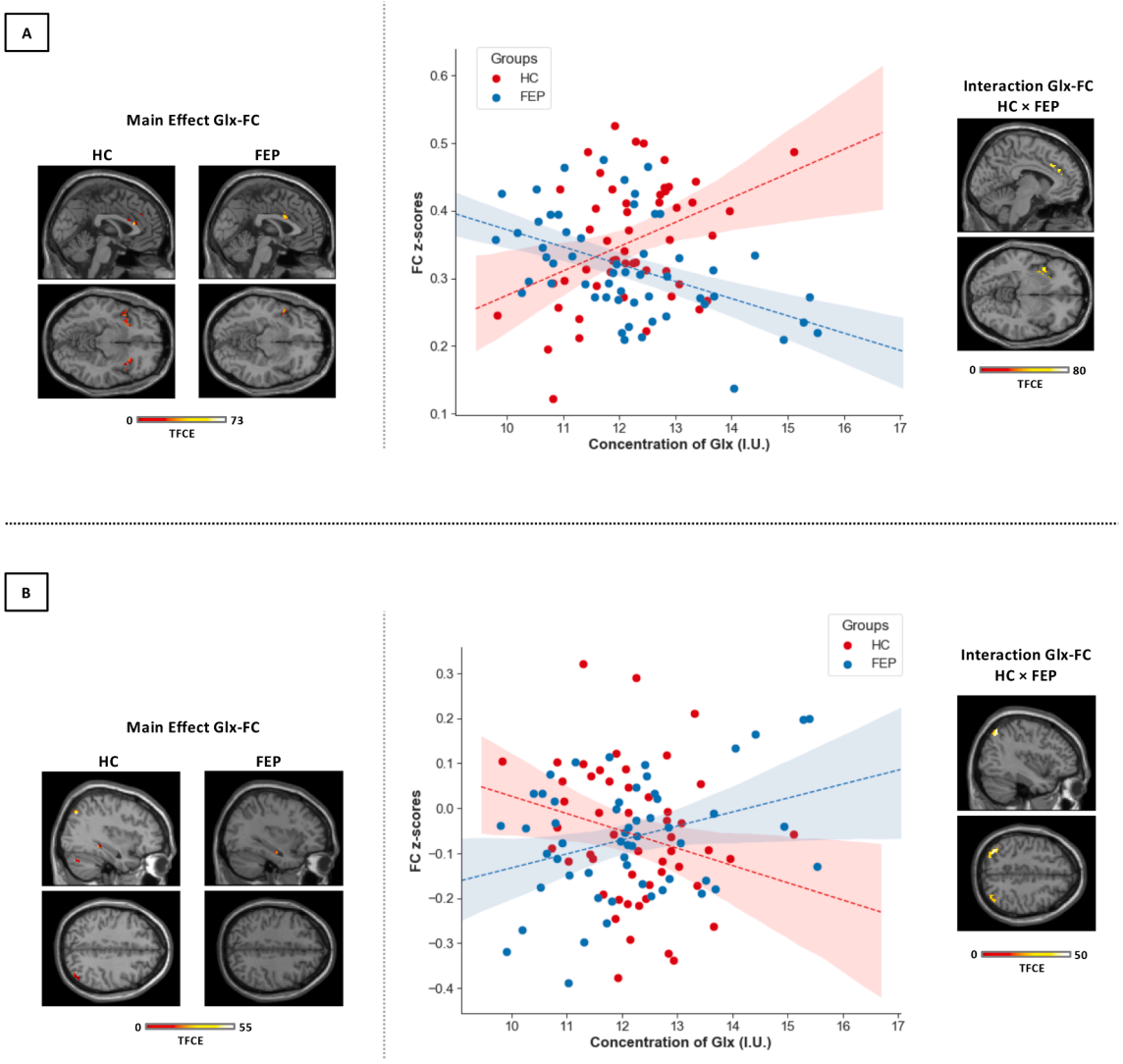

Fig. 3. A) Clusters where main effects and interaction between Glx and FC in the SN mask were found; B) clusters where main effects and interaction between Glx and FC in the SN anticorrelation mask were found. Clusters of group interactions in Glx-FC associations were combined and FC was extracted for data scatterplot visualization purposes. All analyses were TFCE corrected. HC, healthy controls; FEP, first episode psychosis; FC, functional connectivity; dACC, dorsal anterior cingulate cortex; Glx, glutamate + glutamine; TFCE, threshold-free cluster enhancement; and I.U., institutional unit.

controlling for age, gender, and smoking status ($F_{1,\ 115} = 1.30$, $p = 0.26$; Fig. 1B).

1.2.3. *Brain connectivity*

When examining positive FC of the SN, both HC and FEP showed robust connectivity between dACC and bilateral insula, superior frontal, and supramarginal gyrus (Supplementary Table 1 and Supplementary Fig. 1A). When examining negative FC of the SN, both HC and FEP showed anticorrelations between the dACC with precuneus and bilateral angular gyri (Supplementary Table 1 and Supplementary Fig. 1B). Clusters of group differences (HC > FEP) were found in bilateral insula, anterior and middle cingulate, medial frontal areas, caudate nucleus, and bilateral superior frontal gyrus. (TFCE corrected; Table 2 and Fig. 2). When examining negative FC, no between-group differences were found.

1.2.4. *Glx and FC associations*

Within the SN, Glx predicted FC in bilateral insula, putamen, and dACC areas in the HC group. These relationships were less observed in the FEP group (Supplementary Table 2). Group interaction effects were found in the dACC as well as the bilateral insula and putamen where HC showed positive correlations, but FEP showed inverse ones (TFCE corrected, Table 3, Fig. 3A). On the other hand, Glx predicted FC in anticorrelated areas in fusiform and bilateral angular gyri (Supplementary Table 2). Group interaction effects were found in inferior and superior parietal areas where HC showed negative correlations between FC and Glx whereas FEP showed the opposite effect (TFCE corrected, Table 3, Fig. 3b).

1.2.5. *Post-Hoc brain-behavior analysis*

Lastly, exploratory analyses were performed between BPRS scores and dACC Glx scores, however no significant associations emerged in patients (all *p*'s not significant). Additional analyses were performed on the clusters of significant FC group differences (Fig. 2) and Glx-FC association group interactions (Fig. 3A-B), where FC z-scores were extracted from these regions and correlated with BPRS subscales. No significant correlations emerged (all *p*'s not significant).

1.3. *Discussion*

To our knowledge, this is one of the first studies to investigate the role of glutamate metabolism underlying alterations in functional

Table 1
Demographics, clinical measures, and data quality.

	Groups (N = 122)		
	HC (n = 52)	FEP (n = 70)	*P*-value
Demographic variables			
Age (in years)	24.62 ± 6.28	24.03 ± 6.14	0.61
Sex (M/F)	34/18	44/26	0.77
[a]Parental occupation (SES)	4.46 ± 4.32	5.89 ± 4.71	0.33
[b]No. sf smokers (%)	8%	41%	
Smoking (Packs per day)	0.03 ± 0.09	0.24 ± 0.40	<0.001
[c]No. of cannabis users (%)	0%	30%	
Clinical Variables			
Diagnosis			
Schizophrenia	–	35	–
Schizoaffective Disorder	–	11	–
Bipolar disorder with Psychosis	–	3	–
Schizophreniform Disorder	–	4	–
Psychosis NOS	–	13	–
Brief psychotic disorder	–	2	–
Major Depressive Disorder w/ psychosis	–	2	–
Duration of untreated psychosis (in months)	–	21.43 ± 40.19	–
BPRS			
Positive (3-items)	–	11.42 ± 3.38	–
Negative	–	5.87 ± 3.21	–
Total	–	50.16 ± 11.62	–
[d]RBANS			
Immediate Memory	100.21 ± 16.21	81.90 ± 17.83	<0.001
Visuospatial/Constructional	83.94 ± 13.51	75.00 ± 17.92	0.005
Language	98.15 ± 15.89	82.95 ± 16.87	<0.001
Attention	102.53 ± 16.01	80.45 ± 17.01	<0.001
Delayed Memory	91.87 ± 8.86	77.32 ± 15.71	<0.001
Total index	93.38 ± 11.56	74.15 ± 15.89	<0.001
Scan Quality Data			
MRS			
Cramer-Rao lower bands	3.63 ± 0.65	4.37 ± 1.58	0.002
GM fraction	72.18 ± 7.13	72.08 ± 5.56	0.93
WM fraction	12.86 ± 5.92	13.66 ± 6.04	0.47
CSF fraction	14.19 ± 3.95	14.26 ± 3.69	0.92
[e]FC			
Mean motion (in mm)	0.15 ± 0.06	0.19 ± 0.09	0.01
% of volumes after scrubbing	94.98 ± 5.59	91.10 ± 8.82	0.006

Notes: mean ± standard deviation; data available for [a]118 subjects. Ranks determined from Diagnostic Interview for Genetic Studies where a higher rank (lower numerical value) corresponds to higher socioeconomic status (SES); [b]120 subjects; [c]missing data for 8 patients; [d]109 subjects; [e]113 subjects; RBANS = Repeatable Battery for the Assessment of Neuropsychological Status; BPRS = Brief Psychiatric Rating Scale; MRS = magnetic resonance spectroscopy; GM = gray matter; WM = white matter; CSF = cerebrospinal fluid; FC = functional connectivity. P-values are from χ^2 and independent samples-*t* tests for differences between the groups.

Table 2
Clusters of significant group differences in SN FC.

Analysis	Peak Location, Hemisphere	MNI Coordinates x	y	z	Cluster size (in voxels)	TFCE value
Positive FC	Caudate nucleus, L	−8	4	8	194	180
HC > FEP	Caudate nucleus, R	12	8	12	337	169
	Middle frontal gyrus, R	36	34	36	200	160
	Insula, R	44	16	−6	176	155
	Anterior cingulate, R	2	28	16	349	152
	Anterior cingulate, L	−12	26	24	91	143
	Middle frontal gyrus, L	−26	34	36	53	94
	Inferior frontal gyrus, L	−48	18	−6	102	86
	Middle cingulate, R	2	−16	40	17	82
	Middle cingulate, L	−2	−2	34	17	78
Negative FC						
	N/A	N/A	N/A	N/A	N/A	N/A

Abbreviations: SN, salience network; FC, functional connectivity; R, right; L, left; MNI, Montreal Neurological Institute; TFCE, threshold-free cluster enhancement; N/A, not available.

Table 3
Clusters of significant group interactions where Glx was associated with FC.

Analysis	Peak Location, Hemisphere	MNI Coordinates x	y	z	Cluster size (in voxels)	TFCE value
Positive FC						
	Anterior cingulate cortex, R	6	26	32	20	48.41
	Insula, L	−40	12	−6	74	37.87
	Superior medial gyrus, L	−6	36	26	22	37.64
	Superior medial gyrus, L	−8	28	34	43	37.22
	Putamen, L	−30	10	2	28	34.63
Negative FC						
	Inferior parietal lobule, L	−36	−68	46	131	50.59
	Superior parietal lobule, R	36	−74	50	69	32.44

Abbreviations: SN, salience network; FC, functional connectivity; R, right; L, left; MNI, Montreal Neurological Institute; TFCE, threshold-free cluster enhancement.

connectivity of the salience network (SN) in antipsychotic-naïve FEP patients. Compared to HC, in FEP, we found reduced FC in this network in the absence of group differences in dACC Glx levels. Glx-FC group interactions were found in the dACC and bilateral insula for positive FC, and in the lateral parietal cortex for negative FC. In controls, higher Glx levels predicted greater positive FC in dACC and insula, and greater negative FC with regions of the lateral parietal cortex whereas these relationships were weaker or absent in FEP. Our data empirically demonstrate that Glx levels are associated differently with functional connectivity in FEP than in HC, pointing to a possible mechanism underlying dysconnectivity in psychosis.

Contrary to our hypothesis, we found no evidence of excess dACC Glx in antipsychotic-naïve FEP. Nevertheless, our findings are consistent with previous studies where unmedicated patients (Kraguljac et al., 2019; Limongi et al., 2020, 2021), medicated patients (Kraguljac et al., 2012; Merritt et al., 2016) and medication-naïve FEP (Bojesen et al., 2019; Theberge et al., 2002) patients showed no difference in Glx in the dACC compared to HC. Although previous studies have shown reduced glutamate levels in the dACC in FEP (Jeon et al., 2021; Overbeek et al., 2019; Reid et al., 2019; Wang et al., 2019), three of these studies had

medicated FEP subjects and all studies were obtained on a 7 T magnet where the otherwise overlapping of glutamate and glutamine could be resolved, providing separate measures of glutamate and glutamine. Future studies in medication-naïve FEP subjects obtained on a 7 T will be needed to clarify whether glutamate and glutamine are altered in this cohort.

In medication-naïve FEP, we found reduced positive, but not negative, FC of the SN compared to HC. Our findings are generally consistent with network level dysconnectivity evidence in FEP (Gong et al., 2017; Li et al., 2017). Reduced functional connectivity in the SN has been reported in mostly medicated subjects in early stage of illness (Pu et al., 2012) and in chronic patients (Shukla et al., 2019). Overall, reduced within-network functional connectivity (Anhoj et al., 2018; Gong et al., 2017) appears to be a consistent finding in FEP, suggesting an atypical network mechanism of impaired integration and differentiation in FEP (Sepulcre et al., 2012).

Interestingly, in HC, higher Glx levels predicted greater positive FC with hub regions of the SN, and greater negative FC with region of the lateral parietal cortex, suggesting an even greater impact of Glx on brain network dynamics than previously shown as this is one of the first study to evaluate the effect of Glx on both positive and negative functional connectivity. In addition, our finding of dACC Glx predicting FC not only in the dACC but in other brain locations suggests its vital role in regulation of brain connectivity in local and distant regions (Duncan et al., 2014). Our results in HC are consistent with previous studies where Glx was found to positively correlate with the BOLD signal (Duncan and Wiebking et al., 2013; Enzi et al., 2012; Kapogiannis et al., 2013). Additionally, associations between glutamatergic concentration and BOLD signal have been previously observed in the rat brain (Hyder et al., 2006; Smith et al., 2002) suggesting that glutamate may play an essential role in neural activity across species. In the same line, our Glx-FC correlations may be explained from a neuroenergetics framework perspective where positive glucose metabolism (a proxy for brain activity) and glutamatergic activity associations have been previously reported in both animal and human studies (Rothman et al., 2003; Tomasi et al., 2013), which contrasts ours Glx-FC results in FEP where no such correlations were found. The reduced FC in FEP may stem from abnormal glucose metabolism (Amorim et al., 2017; Dean et al., 2016), which then may impact its interaction with Glx.

In sharp contrast, weaker or no correlations between Glx and FC were found in FEP suggesting atypical coupling between these mechanisms, which was later confirmed in our interaction results. While no associations were found between Glx and FC with symptom severity, a more thorough investigation is needed to explore this. Our Glx-FC interaction results are consistent with the results of a recent study showing that healthy controls showed positive correlations between dACC Glx and resting state FC of the SN, whereas medicated schizophrenia patients showed weaker or no correlations (Shukla et al., 2019). This BOLD-MRS interaction has been previously explored with task fMRI using a 7 T magnet (Overbeek et al., 2019) and while their results may seem contradictory to ours, they in fact are comparable. For example, the negative correlations between dACC glutamate and the BOLD Stroop effect in HC in Overbeek and colleagues may reflect an inhibitory mechanism that is parallel to our negative Glx-FC correlations (Fig. 3B) and this is affected in both medicated and unmedicated FEP as they showed a different profile of increased Glx/Glutamate with increased BOLD correlations/Stroop effect. This effect may stem from a compensatory mechanism where reduced FC levels lead to increased Glx levels in FEP (albeit not significantly higher than HC in our study). This effect was observed at both 3T and 7T, nonetheless, future studies should examine both FC and glutamate levels at 7T to corroborate our 3T findings.

Interestingly, previous studies have found strong links between SN FC (using resting state fMRI) and dopamine functioning (using positron emission tomography) in humans. Dopaminergic activity is usually seen during the identification of behaviorally relevant environmental stimuli, similarly to one of the SN's main role, suggesting that dopamine plays a role in modulating SN (McCutcheon et al., 2019). This is of interest given that a similar interaction effect was found when correlating dopamine activity with dACC Glx concentration in FEP patients and HC (Jauhar et al., 2018). This might pinpoint to a biological mechanism where higher concentration of glutamate is related to stronger SN FC/dopamine activity in HC, and this particular mechanism might be impaired in FEP. Finally, postmortem studies of the dACC in schizophrenia have reported both GABA-ergic interneurons alterations (Benes, 2015), as well as decrease in the number of both excitatory and inhibitory synapses (Roberts et al., 2020). Those findings are consistent with recent large scale genome wide association (GWAS) studies in schizophrenia that identified variations in genes involved in synaptic function and neuronal signaling, including those associated with glutamatergic function (Marshall et al., 2017; Schizophrenia Working Group of the Psychiatric Genomics, 2014), as well as with the findings that common-variants identified by those GWAS map to a limited set of neurons, including pyramidal cells and interneurons (Skene et al., 2018). A balance in excitatory/inhibitory mechanisms are thought to regulate the functional integration and segregation of neurons, proving optimal input and output synaptic activity in the brain. Together, our results suggest that Glx robustly integrates regional and long-range connectivity in healthy controls and that this effect is altered in FEP, putatively because of impaired neoroenergetics, dopaminergic and excitatory/inhibitory mechanisms.

Potential strengths and limitations of this study are the following. We enrolled medication-naïve FEP patients who had not been exposed to antipsychotics, which allowed us to study psychosis without medication or illness chronicity confounds. While exposure to cannabis may affect brain functioning and structure, it is considered one of the major risk factors for developing psychosis and consequently remains highly clinically relevant. Excluding patients with history of cannabis would have inadvertently biased our sample and limited the generalizability of our results. Similarly, a small minority of patients were prescribed antidepressants upon study entry, therefore, it is not possible to entirely rule out that serotonergic action may have affected glutamate measurements (Park et al., 2021). While our MRS acquisition sequence does have some drawbacks such as J-modulation, a long echo time, and T2 relaxation effects on the spectrum as well as a water signal that is highly T2 weighted and sensitive to cerebrospinal fluid contamination (Wilson et al., 2019), a significant advantage of these acquisition parameters is that it allows us put findings in context of a number of our previous studies for which we used the same acquisition parameters (Kraguljac et al., 2012, 2019; Reid et al., 2010). Future studies should include larger sample sizes to investigate key clinical implications (such as duration of untreated psychosis, responders and non-responders, different diagnostic profiles, etc.) in order to better characterize the neural correlates of FEP and also have access to stronger magnets to reveal atypical levels of neurotransmitters in psychiatric disorders that 3 T magnets cannot.

1.4. Conclusions

To summarize, we simultaneously investigated Glx concentrations, brain connectivity, and their interaction in the SN in medication-naïve patients with FEP and found intact Glx concentrations, reduced FC, and altered relationship between Glx and FC in FEP compared to HC, suggesting abnormal glutamatergic neurometabolism and brain network connectivity in psychosis. Overall, our findings add to the literature of atypical brain functioning in patients who have just begun experiencing the detrimental effects of psychosis and highlight the need for immediate treatment after experiencing the initial symptoms to better long-term clinical outcomes.

Declaration of Competing Interest

The authors declare that they have no known competing financial interests or personal relationships that could have appeared to influence the work reported in this paper.

Acknowledgement

Special thanks to the patients and their families.

Funding

This work was supported by the National Institutes of Health (R01MH102951 and R01MH113800).

Clinical trial registration

Trajectories of Treatment Response as Window into the Heterogeneity of Psychosis: A Longitudinal Multimodal Imaging Study, NCT03442101 https://clinicaltrials.gov/ct2/show/NCT03442101.

Glutamate, Brain Connectivity and Duration of Untreated Psychosis (DUP), NCT02034253 https://clinicaltrials.gov/ct2/show/NCT02034253.

Role of the Sponsor

The funding agency had no role in the design and conduct of the study; collection, management, analysis, and interpretation of the data; and preparation, review, or approval of the manuscript; and decision to submit the manuscript for publication.

Author Contributions

Dr. Lahti had full access to all of the data in the study and takes responsibility for the integrity of the data and the accuracy of the data analysis.

Study concept and design

ACL.

Acquisition of data

WPA, NVK.

Analysis and interpretation of data

All authors.

Drafting of the manuscript

JOM, FMB, NVK, ACL.

Statistical analysis

JOM.

Obtained funding

ACL.

Administrative, technical, or material support

ACL.

Study supervision

ACL.

Appendix A. Supplementary data

Supplementary data to this article can be found online at https://doi.org/10.1016/j.nicl.2021.102845.

References

Amorim, M., Moreira, A., Marques, A., Summavielle, T., 2017. Brain metabolic abnormalities in schizophrenia patients. Eur. Psychiatry 41 (S1), s802.

Anhoj, S., Odegaard Nielsen, M., Jensen, M.H., Ford, K., Fagerlund, B., Williamson, P., Rostrup, E., 2018. Alterations of Intrinsic Connectivity Networks in Antipsychotic-Naive First-Episode Schizophrenia. Schizophr. Bull. 44 (6), 1332–1340. https://doi.org/10.1093/schbul/sbx171.

Benes, F.M., 2015. The GABA system in schizophrenia: cells, molecules and microcircuitry. Schizophr. Res. 167 (1–3), 1–3. https://doi.org/10.1016/j.schres.2015.07.017.

Bojesen, K.B., Ebdrup, B.H., Jessen, K., Sigvard, A., Tangmose, K., Edden, R.A.E., Glenthoj, B.Y., 2019. Treatment response after 6 and 26 weeks is related to baseline glutamate and GABA levels in antipsychotic-naive patients with psychosis. Psychol. Med. 1–12 https://doi.org/10.1017/S0033291719002277.

Briend, F., Nelson, E.A., Maximo, O., Armstrong, W.P., Kraguljac, N.V., Lahti, A.C., 2020. Hippocampal glutamate and hippocampus subfield volumes in antipsychotic-naive first episode psychosis subjects and relationships to duration of untreated psychosis. Transl. Psychiatry 10 (1), 137. https://doi.org/10.1038/s41398-020-0812-z.

Cadena, E.J., White, D.M., Kraguljac, N.V., Reid, M.A., Lahti, A.C., 2018a. Evaluation of fronto-striatal networks during cognitive control in unmedicated patients with schizophrenia and the effect of antipsychotic medication. NPJ Schizophr. 4 (1), 8. https://doi.org/10.1038/s41537-018-0051-y.

Cadena, E.J., White, D.M., Kraguljac, N.V., Reid, M.A., Maximo, J.O., Nelson, E.A., Gawronski, B.A., Lahti, A.C., 2018b. A longitudinal multimodal neuroimaging study to examine relationships between resting state glutamate and task related BOLD response in schizophrenia. Front. Psychiatry 9. https://doi.org/10.3389/fpsyt.2018.00632.

Cadena, E.J., White, D.M., Kraguljac, N.V., Reid, M.A., Jindal, R., Pixley, R.M., Lahti, A.C., 2019. Cognitive control network dysconnectivity and response to antipsychotic treatment in schizophrenia. Schizophr. Res. 204, 262–270. https://doi.org/10.1016/j.schres.2018.07.045.

Carpenter Jr., W.T., Gold, J.M., Lahti, A.C., Queern, C.A., Conley, R.R., Bartko, J.J., Appelbaum, P.S., 2000. Decisional capacity for informed consent in schizophrenia research. Arch. Gen. Psychiatry 57 (6), 533–538. https://doi.org/10.1001/archpsyc.57.6.533.

de la Fuente-Sandoval, C., León-Ortiz, P., Azcárraga, M., Stephano, S., Favila, R., Díaz-Galvis, L., Alvarado-Alanis, P., Ramírez-Bermúdez, J., Graff-Guerrero, A., 2013. Glutamate levels in the associative striatum before and after 4 weeks of antipsychotic treatment in first-episode psychosis: a longitudinal proton magnetic resonance spectroscopy study. JAMA Psychiatry 70 (10), 1057. https://doi.org/10.1001/jamapsychiatry.2013.289.

Dean, B., Thomas, N., Scarr, E., Udawela, M., 2016. Evidence for impaired glucose metabolism in the striatum, obtained postmortem, from some subjects with schizophrenia. Transl. Psychiatry 6 (11), e949. https://doi.org/10.1038/tp.2016.226.

Dempster, K., Jeon, P., MacKinley, M., Williamson, P., Theberge, J., Palaniyappan, L., 2020. Early treatment response in first episode psychosis: a 7-T magnetic resonance spectroscopic study of glutathione and glutamate. Mol. Psychiatry 25 (8), 1640–1650. https://doi.org/10.1038/s41380-020-0704-x.

Duncan, N.W., Wiebking, C., Tiret, B., Marjanska, M., Hayes, D.J., Lyttleton, O., Northoff, G., 2013. Glutamate concentration in the medial prefrontal cortex predicts resting-state cortical-subcortical functional connectivity in humans. PLoS ONE 8 (4), e60312. https://doi.org/10.1371/journal.pone.0060312.

Duncan, N.W., Wiebking, C., Northoff, G., 2014. Associations of regional GABA and glutamate with intrinsic and extrinsic neural activity in humans-a review of multimodal imaging studies. Neurosci. Biobehav. Rev. 47, 36–52. https://doi.org/10.1016/j.neubiorev.2014.07.016.

Egerton, A., Modinos, G., Ferrera, D., McGuire, P., 2017. Neuroimaging studies of GABA in schizophrenia: a systematic review with meta-analysis. Transl. Psychiatry 7 (6), e1147. https://doi.org/10.1038/tp.2017.124.

Enzi, B., Duncan, N.W., Kaufmann, J., Tempelmann, C., Wiebking, C., Northoff, G., 2012. Glutamate modulates resting state activity in the perigenual anterior cingulate cortex - a combined fMRI-MRS study. Neuroscience 227, 102–109. https://doi.org/10.1016/j.neuroscience.2012.09.039.

Falkenberg, L.E., Westerhausen, R., Craven, A.R., Johnsen, E., Kroken, R.A., L∅berg, E.-M., Specht, K., Hugdahl, K., 2014. Impact of glutamate levels on neuronal response and cognitive abilities in schizophrenia. Neuroimage Clin. 4, 576–584. https://doi.org/10.1016/j.nicl.2014.03.014.

Gasparovic, C., Song, T., Devier, D., Bockholt, H.J., Caprihan, A., Mullins, P.G., Posse, S., Jung, R.E., Morrison, L.A., 2006. Use of tissue water as a concentration reference for proton spectroscopic imaging. Magn. Reson. Med. 55 (6), 1219–1226. https://doi.org/10.1002/mrm.20901.

Goelman, G., Gordon, N., Bonne, O., Gozzi, A., 2014. Maximizing negative correlations in resting-state functional connectivity MRI by time-lag. PLoS ONE 9 (11), e111554. https://doi.org/10.1371/journal.pone.0111554.

Gong, Q., Hu, X., Pettersson-Yeo, W., Xu, X., Lui, S., Crossley, N., Mechelli, A., 2017. Network-level dysconnectivity in drug-naive first-episode psychosis: dissociating transdiagnostic and diagnosis-specific alterations. Neuropsychopharmacology 42 (4), 933–940. https://doi.org/10.1038/npp.2016.247.

Gussew, A., Erdtel, M., Hiepe, P., Rzanny, R., Reichenbach, J.R., 2012. Absolute quantitation of brain metabolites with respect to heterogeneous tissue compositions in (1)H-MR spectroscopic volumes. MAGMA 25 (5), 321–333. https://doi.org/10.1007/s10334-012-0305-z.

Hyder, F., Patel, A.B., Gjedde, A., Rothman, D.L., Behar, K.L., Shulman, R.G., 2006. Neuronal-glial glucose oxidation and glutamatergic-GABAergic function. J. Cereb. Blood Flow Metab. 26 (7), 865–877. https://doi.org/10.1038/sj.jcbfm.9600263.

Jauhar, S., McCutcheon, R., Borgan, F., Veronese, M., Nour, M., Pepper, F., Rogdaki, M., Stone, J., Egerton, A., Turkheimer, F., McGuire, P., Howes, O.D., 2018. The relationship between cortical glutamate and striatal dopamine in first-episode psychosis: a cross-sectional multimodal PET and magnetic resonance spectroscopy imaging study. Lancet Psychiatry 5 (10), 816–823. https://doi.org/10.1016/S2215-0366(18)30268-2.

Jenkinson, M., Beckmann, C.F., Behrens, T.E.J., Woolrich, M.W., Smith, S.M., 2012. Fsl. Neuroimage 62 (2), 782–790. https://doi.org/10.1016/j.neuroimage.2011.09.015.

Jeon, P., Limongi, R., Ford, S.D., MacKinley, M., Dempster, K., Theberge, J., Palaniyappan, L., 2021. Progressive changes in glutamate concentration in early stages of schizophrenia: a longitudinal 7-tesla MRS study. Schizophr. Bull. Open 2 (1), sgaa072.

Kapogiannis, D., Reiter, D.A., Willette, A.A., Mattson, M.P., 2013. Posteromedial cortex glutamate and GABA predict intrinsic functional connectivity of the default mode network. Neuroimage 64, 112–119. https://doi.org/10.1016/j.neuroimage.2012.09.029.

Kapur, S., 2003. Psychosis as a state of aberrant salience: a framework linking biology, phenomenology, and pharmacology in schizophrenia. Am. J. Psychiatry 160 (1), 13–23. https://doi.org/10.1176/appi.ajp.160.1.13.

Kerns, J.G., Cohen, J.D., MacDonald 3rd, A.W., Johnson, M.K., Stenger, V.A., Aizenstein, H., Carter, C.S., 2005. Decreased conflict- and error-related activity in the anterior cingulate cortex in subjects with schizophrenia. Am. J. Psychiatry 162 (10), 1833–1839. https://doi.org/10.1176/appi.ajp.162.10.1833.

Kraguljac, N.V., Reid, M.A., White, D.M., den Hollander, J., Lahti, A.C., 2012. Regional decoupling of N-acetyl-aspartate and glutamate in schizophrenia. Neuropsychopharmacology 37 (12), 2635–2642. https://doi.org/10.1038/npp.2012.126.

Kraguljac, N.V., White, D.M., Reid, M.A., Lahti, A.C., 2013. Increased hippocampal glutamate and volumetric deficits in unmedicated patients with schizophrenia. JAMA Psychiatry 70 (12), 1294–1302. https://doi.org/10.1001/jamapsychiatry.2013.2437.

Kraguljac, N.V., White, D.M., Hadley, J.A., Visscher, K., Knight, D., ver Hoef, L., Falola, B., Lahti, A.C., 2016. Abnormalities in large scale functional networks in unmedicated patients with schizophrenia and effects of risperidone. Neuroimage Clin. 10, 146–158. https://doi.org/10.1016/j.nicl.2015.11.015.

Kraguljac, N.V., Frölich, M.A., Tran, S., White, D.M., Nichols, N., Barton-McArdle, A., Reid, M.A., Bolding, M.S., Lahti, A.C., 2017. Ketamine modulates hippocampal neurochemistry and functional connectivity: a combined magnetic resonance spectroscopy and resting-state fMRI study in healthy volunteers. Mol. Psychiatry 22 (4), 562–569. https://doi.org/10.1038/mp.2016.122.

Kraguljac, N.V., Morgan, C.J., Reid, M.A., White, D.M., Jindal, R.D., Sivaraman, S., Martinak, B.K., Lahti, A.C., 2019. A longitudinal magnetic resonance spectroscopy study investigating effects of risperidone in the anterior cingulate cortex and hippocampus in schizophrenia. Schizophr. Res. 210, 239–244. https://doi.org/10.1016/j.schres.2018.12.028.

Kraguljac, N.V., Lahti, A.C., 2021. Neuroimaging as a window into the pathophysiological mechanisms of schizophrenia. Front. Psychiatry 12, 613764. https://doi.org/10.3389/fpsyt.2021.613764.

Kraguljac, N.V., Anthony, T., Morgan, C.J., Jindal, R.D., Burger, M.S., Lahti, A.C., 2020. White matter integrity, duration of untreated psychosis, and antipsychotic treatment response in medication-naive first-episode psychosis patients. Mol. Psychiatry. https://doi.org/10.1038/s41380-020-0765-x.

Kraguljac, N.V., Monroe, W.S., Anthony, T., Jindal, R.D., Hill, H., Lahti, A.C., 2021. Neurite orientation dispersion and density imaging (NODDI) and duration of untreated psychosis in antipsychotic medication-naïve first episode psychosis patients. Neuroimage Rep. 1 (1), 100005. https://doi.org/10.1016/j.ynirp.2021.100005.

Li, T., Wang, Q., Zhang, J., Rolls, E.T., Yang, W., Palaniyappan, L., Feng, J., 2017. Brain-wide analysis of functional connectivity in first-episode and chronic stages of schizophrenia. Schizophr. Bull. 43 (2), 436–448. https://doi.org/10.1093/schbul/sbw099.

Limongi, R., Jeon, P., Mackinley, M., Das, T., Dempster, K., Théberge, J., Bartha, R., Wong, D., Palaniyappan, L., 2020. Glutamate and dysconnection in the salience network: neurochemical, effective connectivity, and computational evidence in schizophrenia. Biol. Psychiatry 88 (3), 273–281. https://doi.org/10.1016/j.biopsych.2020.01.021.

Limongi, R., Jeon, P., Théberge, J., Palaniyappan, L., 2021. Counteracting effects of glutathione on the glutamate-driven excitation/inhibition imbalance in first-episode schizophrenia: a 7T MRS and dynamic causal modeling study. Antioxidants (Basel) 10 (1), 75. https://doi.org/10.3390/antiox10010075.

Marshall, C.R., Howrigan, D.P., Merico, D., Thiruvahindrapuram, B., Wu, W., Greer, D.S., Antaki, D., Shetty, A., Holmans, P.A., Pinto, D., Gujral, M., Brandler, W.M., Malhotra, D., Wang, Z., Fajarado, K.V.F., Maile, M.S., Ripke, S., Agartz, I., Albus, M., Alexander, M., Amin, F., Atkins, J., Bacanu, S.A., Belliveau, R.A., Bergen, S.E., Bertalan, M., Bevilacqua, E., Bigdeli, T.B., Black, D.W., Bruggeman, R., Buccola, N. G., Buckner, R.L., Bulik-Sullivan, B., Byerley, W., Cahn, W., Cai, G., Cairns, M.J., Campion, D., Cantor, R.M., Carr, V.J., Carrera, N., Catts, S.V., Chambert, K.D., Cheng, W., Cloninger, C.R., Cohen, D., Cormican, P., Craddock, N., Crespo-Facorro, B., Crowley, J.J., Curtis, D., Davidson, M., Davis, K.L., Degenhardt, F., Del Favero, J., DeLisi, L.E., Dikeos, D., Dinan, T., Djurovic, S., Donohoe, G., Drapeau, E., Duan, J., Dudbridge, F., Eichhammer, P., Eriksson, J., Escott-Price, V., Essioux, L., Fanous, A.H., Farh, K.-H., Farrell, M.S., Frank, J., Franke, L., Freedman, R., Freimer, N.B., Friedman, J.I., Forstner, A.J., Fromer, M., Genovese, G., Georgieva, L., Gershon, E.S., Giegling, I., Giusti-Rodríguez, P., Godard, S., Goldstein, J.I., Gratten, J., de Haan, L., Hamshere, M.L., Hansen, M., Hansen, T., Haroutunian, V., Hartmann, A.M., Henskens, F.A., Herms, S., Hirschhorn, J.N., Hoffmann, P., Hofman, A., Huang, H., Ikeda, M., Joa, I., Kähler, A.K., Kahn, R.S., Kalaydjieva, L., Karjalainen, J., Kavanagh, D., Keller, M.C., Kelly, B.J., Kennedy, J.L., Kim, Y., Knowles, J.A., Konte, B., Laurent, C., Lee, P., Lee, S.H., Legge, S.E., Lerer, B., Levy, D. L., Liang, K.-Y., Lieberman, J., Lönnqvist, J., Loughland, C.M., Magnusson, P.K.E., Maher, B.S., Maier, W., Mallet, J., Mattheisen, M., Mattingsdal, M., McCarley, R.W., McDonald, C., McIntosh, A.M., Meier, S., Meijer, C.J., Melle, I., Mesholam-Gately, R. I., Metspalu, A., Michie, P.T., Milani, L., Milanova, V., Mokrab, Y., Morris, D.W., Müller-Myhsok, B., Murphy, K.C., Murray, R.M., Myin-Germeys, I., Nenadic, I., Nertney, D.A., Nestadt, G., Nicodemus, K.K., Nisenbaum, L., Nordin, A., O'Callaghan, E., O'Dushlaine, C., Oh, S.-Y., Olincy, A., Olsen, L., O'Neill, F.A., Van Os, J., Pantelis, C., Papadimitriou, G.N., Parkhomenko, E., Pato, M.T., Paunio, T., Perkins, D.O., Pers, T.H., Pietiläinen, O., Pimm, J., Pocklington, A.J., Powell, J., Price, A., Pulver, A.E., Purcell, S.M., Quested, D., Rasmussen, H.B., Reichenberg, A., Reimers, M.A., Richards, A.L., Roffman, J.L., Roussos, P., Ruderfer, D.M., Salomaa, V., Sanders, A.R., Savitz, A., Schall, U., Schulze, T.G., Schwab, S.G., Scolnick, E.M., Scott, R.J., Seidman, L.J., Shi, J., Silverman, J.M., Smoller, J.W., Söderman, E., Spencer, C.C.A., Stahl, E.A., Strengman, E., Strohmaier, J., Stroup, T. S., Suvisaari, J., Svrakic, D.M., Szatkiewicz, J.P., Thirumalai, S., Tooney, P.A., Veijola, J., Visscher, P.M., Waddington, J., Walsh, D., Webb, B.T., Weiser, M., Wildenauer, D.B., Williams, N.M., Williams, S., Witt, S.H., Wolen, A.R., Wormley, B. K., Wray, N.R., Wu, J.Q., Zai, C.C., Adolfsson, R., Andreassen, O.A., Blackwood, D.H. R., Bramon, E., Buxbaum, J.D., Cichon, S., Collier, D.A., Corvin, A., Daly, M.J., Darvasi, A., Domenici, E., Esko, T., Gejman, P.V., Gill, M., Gurling, H., Hultman, C. M., Iwata, N., Jablensky, A.V., Jönsson, E.G., Kendler, K.S., Kirov, G., Knight, J.o., Levinson, D.F., Li, Q.S., McCarroll, S.A., McQuillin, A., Moran, J.L., Mowry, B.J., Nöthen, M.M., Ophoff, R.A., Owen, M.J., Palotie, A., Pato, C.N., Petryshen, T.L., Posthuma, D., Rietschel, M., Riley, B.P., Rujescu, D., Sklar, P., St Clair, D., Walters, J. T.R., Werge, T., Sullivan, P.F., O'Donovan, M.C., Scherer, S.W., Neale, B.M., Sebat, J., 2017. Contribution of copy number variants to schizophrenia from a genome-wide study of 41,321 subjects. Nat. Genet. 49 (1), 27–35. https://doi.org/10.1038/ng.3725.

Maximo, J.O., Nelson, E.A., Armstrong, W.P., Kraguljac, N.V., Lahti, A.C., 2020. Duration of untreated psychosis correlates with brain connectivity and morphology in medication-naive patients with first-episode psychosis. Biol. Psychiatry Cogn. Neurosci. Neuroimaging 5 (2), 231–238. https://doi.org/10.1016/j.bpsc.2019.10.014.

McCutcheon, R.A., Nour, M.M., Dahoun, T., Jauhar, S., Pepper, F., Expert, P., Veronese, M., Adams, R.A., Turkheimer, F., Mehta, M.A., Howes, O.D., 2019. Mesolimbic dopamine function is related to salience network connectivity: an integrative positron emission tomography and magnetic resonance study. Biol. Psychiatry 85 (5), 368–378.

McCutcheon, R.A., Pillinger, T., Rogdaki, M., Bustillo, J., Howes, O.D., 2021. Glutamate connectivity associations converge upon the salience network in schizophrenia and healthy controls. Transl. Psychiatry 11 (1), 322. https://doi.org/10.1038/s41398-021-01455-y.

Menon, V., 2011. Large-scale brain networks and psychopathology: a unifying triple network model. Trends Cogn Sci 15 (10), 483–506. https://doi.org/10.1016/j.tics.2011.08.003.

Merritt, K., Egerton, A., Kempton, M.J., Taylor, M.J., McGuire, P.K., 2016. Nature of glutamate alterations in schizophrenia: a meta-analysis of proton magnetic resonance spectroscopy studies. JAMA Psychiatry 73 (7), 665–674. https://doi.org/10.1001/jamapsychiatry.2016.0442.

Minzenberg, M.J., Laird, A.R., Thelen, S., Carter, C.S., Glahn, D.C., 2009. Meta-analysis of 41 functional neuroimaging studies of executive function in schizophrenia. Arch. Gen. Psychiatry 66 (8), 811–822. https://doi.org/10.1001/archgenpsychiatry.2009.91.

Mullins, P.G., Chen, H., Xu, J., Caprihan, A., Gasparovic, C., 2008. Comparative reliability of proton spectroscopy techniques designed to improve detection of J-coupled metabolites. Magn. Reson. Med. 60 (4), 964–969. https://doi.org/10.1002/mrm.v60:410.1002/mrm.21696.

Murphy, K., Birn, R.M., Handwerker, D.A., Jones, T.B., Bandettini, P.A., 2009. The impact of global signal regression on resting state correlations: are anti-correlated networks introduced? Neuroimage 44 (3), 893–905. https://doi.org/10.1016/j.neuroimage.2008.09.036.

Nelson, E.A., Kraguljac, N.V., Maximo, J.O., Briend, F., Armstrong, W., Ver Hoef, L.W., Lahti, A.C., 2020. Hippocampal dysconnectivity and altered glutamatergic modulation of the default mode network: a combined resting-state connectivity and magnetic resonance spectroscopy study in schizophrenia. Biol. Psychiatry Cogn. Neurosci. Neuroimag. https://doi.org/10.1016/j.bpsc.2020.04.014.

Overall, J.E., Gorham, D.R., 1962. The brief psychiatric rating scale. Psychol. Rep. 10 (3), 799–812.

Overbeek, G., Gawne, T.J., Reid, M.A., Salibi, N., Kraguljac, N.V., White, D.M., Lahti, A. C., 2019. Relationship between cortical excitation and inhibition and task-induced activation and deactivation: a combined magnetic resonance spectroscopy and functional magnetic resonance imaging study at 7T in first-episode psychosis. Biol Psychiatry Cogn Neurosci Neuroimaging 4 (2), 121–130. https://doi.org/10.1016/j.bpsc.2018.10.002.

Pan, Y., Dempster, K., Jeon, P., Theberge, J., Khan, A.R., Palaniyappan, L., 2021. Acute conceptual disorganization in untreated first-episode psychosis: a combined magnetic resonance spectroscopy and diffusion imaging study of the cingulum. J. Psychiatry Neurosci. 46 (3), E337–E346. https://doi.org/10.1503/jpn.200167.

Park, M.T.M., Jeon, P., Khan, A.R., Dempster, K., Chakravarty, M.M., Lerch, J.P., MacKinley, M., Théberge, J., Palaniyappan, L., 2021. Hippocampal neuroanatomy in first episode psychosis: a putative role for glutamate and serotonin receptors. Prog. Neuro-Psychopharmacol. Biol. Psychiatry 110, 110297. https://doi.org/10.1016/j.pnpbp.2021.110297.

Pu, W., Li, L.i., Zhang, H., Ouyang, X., Liu, H., Zhao, J., Li, L., Xue, Z., Xu, K.e., Tang, H., Shan, B., Liu, Z., Wang, F., 2012. Morphological and functional abnormalities of salience network in the early-stage of paranoid schizophrenia. Schizophr. Res. 141 (1), 15–21. https://doi.org/10.1016/j.schres.2012.07.017.

Randolph, C., Tierney, M.C., Mohr, E., Chase, T.N., 1998. The repeatable battery for the assessment of neuropsychological status (RBANS): preliminary clinical validity. J. Clin. Exp. Neuropsychol. 20 (3), 310–319. https://doi.org/10.1076/jcen.20.3.310.823.

Reid, M.A., Stoeckel, L.E., White, D.M., Avsar, K.B., Bolding, M.S., Akella, N.S., Knowlton, R.C., den Hollander, J.A., Lahti, A.C., 2010. Assessments of function and biochemistry of the anterior cingulate cortex in schizophrenia. Biol. Psychiatry 68 (7), 625–633. https://doi.org/10.1016/j.biopsych.2010.04.013.

Reid, M.A., Salibi, N., White, D.M., Gawne, T.J., Denney, T.S., Lahti, A.C., 2019. 7T proton magnetic resonance spectroscopy of the anterior cingulate cortex in first-episode schizophrenia. Schizophr. Bull. 45 (1), 180–189. https://doi.org/10.1093/schbul/sbx190.

Roberts, R.C., McCollum, L.A., Schoonover, K.E., Mabry, S.J., Roche, J.K., Lahti, A.C., 2020. Ultrastructural evidence for glutamatergic dysregulation in schizophrenia. Schizophr. Res. https://doi.org/10.1016/j.schres.2020.01.016.

Rothman, D.L., Behar, K.L., Hyder, F., Shulman, R.G., 2003. In vivo NMR studies of the glutamate neurotransmitter flux and neuroenergetics: implications for brain function. Annu. Rev. Physiol. 65 (1), 401–427. https://doi.org/10.1146/annurev.physiol.65.092101.142131.

Scheidegger, O., Wingeier, K., Stefan, D., Graveron-Demilly, D., van Ormondt, D., Wiest, R., Slotboom, J., 2013. Optimized quantitative magnetic resonance spectroscopy for clinical routine. Magn. Reson. Med. 70 (1), 25–32. https://doi.org/10.1002/mrm.v70.110.1002/mrm.24455.

Schizophrenia Working Group of the Psychiatric Genomics, C, 2014. Biological insights from 108 schizophrenia-associated genetic loci. Nature 511 (7510), 421–427. https://doi.org/10.1038/nature13595.

Schubert, F., Gallinat, J., Seifert, F., Rinneberg, H., 2004. Glutamate concentrations in human brain using single voxel proton magnetic resonance spectroscopy at 3 Tesla. Neuroimage 21 (4), 1762–1771. https://doi.org/10.1016/j.neuroimage.2003.11.014.

Sepulcre, J., Sabuncu, M.R., Johnson, K.A., 2012. Network assemblies in the functional brain. Curr. Opin. Neurol. 25 (4), 384–391. https://doi.org/10.1097/WCO.0b013e328355a8e8.

Shukla, D.K., Wijtenburg, S.A., Chen, H., Chiappelli, J.J., Kochunov, P., Hong, L.E., Rowland, L.M., 2019. Anterior cingulate glutamate and GABA associations on functional connectivity in schizophrenia. Schizophr. Bull. 45 (3), 647–658. https://doi.org/10.1093/schbul/sby075.

Shulman, R.G., Hyder, F., Rothman, D.L., 2014. Insights from neuroenergetics into the interpretation of functional neuroimaging: an alternative empirical model for studying the brain's support of behavior. J. Cereb. Blood Flow Metab. 34 (11), 1721–1735. https://doi.org/10.1038/jcbfm.2014.145.

Singh, K.D., 2012. Which "neural activity" do you mean? fMRI, MEG, oscillations and neurotransmitters. Neuroimage 62 (2), 1121–1130. https://doi.org/10.1016/j.neuroimage.2012.01.028.

Skene, N.G., Bryois, J., Bakken, T.E., Breen, G., Crowley, J.J., Gaspar, Héléna.A., Giusti-Rodriguez, P., Hodge, R.D., Miller, J.A., Muñoz-Manchado, A.B., O'Donovan, M.C., Owen, M.J., Pardiñas, A.F., Ryge, J., Walters, J.T.R., Linnarsson, S., Lein, E.S., Sullivan, P.F., Hjerling-Leffler, J., 2018. Genetic identification of brain cell types underlying schizophrenia. Nat. Genet. 50 (6), 825–833. https://doi.org/10.1038/s41588-018-0129-5.

Smith, A.J., Blumenfeld, H., Behar, K.L., Rothman, D.L., Shulman, R.G., Hyder, F., 2002. Cerebral energetics and spiking frequency: the neurophysiological basis of fMRI. Proc. Natl. Acad. Sci. U.S.A. 99 (16), 10765–10770. https://doi.org/10.1073/pnas.132272199.

Smith, S.M., Nichols, T.E., 2009. Threshold-free cluster enhancement: addressing problems of smoothing, threshold dependence and localisation in cluster inference. Neuroimage 44 (1), 83–98. https://doi.org/10.1016/j.neuroimage.2008.03.061.

Stone, J.M., Day, F., Tsagaraki, H., Valli, I., McLean, M.A., Lythgoe, D.J., O'Gorman, R.L., Barker, G.J., McGuire, P.K., 2009. Glutamate dysfunction in people with prodromal symptoms of psychosis: relationship to gray matter volume. Biol. Psychiatry 66 (6), 533–539. https://doi.org/10.1016/j.biopsych.2009.05.006.

Sydnor, V.J., Roalf, D.R., 2020. A meta-analysis of ultra-high field glutamate, glutamine, GABA and glutathione 1HMRS in psychosis: Implications for studies of psychosis risk. Schizophr. Res. 226, 61–69. https://doi.org/10.1016/j.schres.2020.06.028.

Theberge, J., Bartha, R., Drost, D.J., Menon, R.S., Malla, A., Takhar, J., Williamson, P.C., 2002. Glutamate and glutamine measured with 4.0 T proton MRS in never-treated patients with schizophrenia and healthy volunteers. Am. J. Psychiatry 159 (11), 1944–1946. https://doi.org/10.1176/appi.ajp.159.11.1944.

Tomasi, D., Wang, G.J., Volkow, N.D., 2013. Energetic cost of brain functional connectivity. Proc. Natl. Acad. Sci. U.S.A. 110 (33), 13642–13647. https://doi.org/10.1073/pnas.1303346110.

Vanhamme, L., van den Boogaart, A., Van Huffel, S., 1997. Improved method for accurate and efficient quantification of MRS data with use of prior knowledge. J. Magn. Reson. 129 (1), 35–43. https://doi.org/10.1006/jmre.1997.1244.

Wang, A.M., Pradhan, S., Coughlin, J.M., Trivedi, A., DuBois, S.L., Crawford, J.L., Sedlak, T.W., Nucifora, F.C., Nestadt, G., Nucifora, L.G., Schretlen, D.J., Sawa, A., Barker, P.B., 2019. Assessing brain metabolism with 7-T proton magnetic resonance spectroscopy in patients with first-episode psychosis. JAMA Psychiatry 76 (3), 314. https://doi.org/10.1001/jamapsychiatry.2018.3637.

Whitfield-Gabrieli, S., Nieto-Castanon, A., 2012. Conn: a functional connectivity toolbox for correlated and anticorrelated brain networks. Brain Connect. 2 (3), 125–141. https://doi.org/10.1089/brain.2012.0073.

Williamson, P.C., Allman, J.M., 2012. A framework for interpreting functional networks in schizophrenia. Front. Hum. Neurosci. 6, 184. https://doi.org/10.3389/fnhum.2012.00184.

Wilson, M., Andronesi, O., Barker, P.B., Bartha, R., Bizzi, A., Bolan, P.J., Brindle, K.M., Choi, I., Cudalbu, C., Dydak, U., Emir, U.E., Gonzalez, R.G., Gruber, S., Gruetter, R., Gupta, R.K., Heerschap, A., Henning, A., Hetherington, H.P., Huppi, P.S., Hurd, R.E., Kantarci, K., Kauppinen, R.A., Klomp, D.W.J., Kreis, R., Kruiskamp, M.J., Leach, M. O., Lin, A.P., Luijten, P.R., Marjańska, M., Maudsley, A.A., Meyerhoff, D.J., Mountford, C.E., Mullins, P.G., Murdoch, J.B., Nelson, S.J., Noeske, R., Öz, Gülin, Pan, J.W., Peet, A.C., Poptani, H., Posse, S., Ratai, E., Salibi, N., Scheenen, T.W.J., Smith, I.C.P., Soher, B.J., Tkáč, I., Vigneron, D.B., Howe, F.A., 2019. Methodological consensus on clinical proton MRS of the brain: Review and recommendations. Magn. Reson. Med. 82 (2), 527–550. https://doi.org/10.1002/mrm.v82.210.1002/mrm.27742.